



Case Report Genitourinary and Gynecologic Imaging

# Granulomatous prostatitis following Bacillus Calmette–Guérin therapy

Siddhi Hegde<sup>1</sup>, Dhairya A. Lakhani<sup>2</sup>, Ion Prisneac<sup>3</sup>, Brian Markovich<sup>2</sup>

<sup>1</sup>Department of Radiology, Massachusetts General Hospital, Boston, Departments of <sup>2</sup>Radiology and <sup>3</sup>Pathology, Anatomy and Laboratory Medicine, West Virginia University, Morgantown, United States.



\*Corresponding author:  
Siddhi Hegde,  
Department of Radiology,  
Massachusetts General  
Hospital, Boston, United States.  
siddhi.hegde5@gmail.com

Received: 16 May 2023  
Accepted: 26 June 2024  
Published: 17 October 2024

DOI  
10.25259/JCIS\_47\_2023

Quick Response Code:



## ABSTRACT

Granulomatous prostatitis (GP) is a rare form of chronic prostatitis with reported incidence of 0.65–1.5%. Radiological features of GP overlap with those of prostate adenocarcinoma. The following magnetic resonance imaging characteristics can suggest the diagnosis in an appropriate clinical setting: Diffuse or focal nodular low T2 signal, high signal on diffusion-weighted imaging with corresponding low apparent diffusion coefficient signal, and post-contrast imaging with lesion enhancement or rim-enhancing in the setting of caseous necrosis or abscess formation. Even with suspicion on imaging, the overlapping imaging features with prostate adenocarcinoma necessitate biopsy for confirmatory diagnosis. Here, we report a case of a 70-year-old man with GP in the setting of prior intravesicle bacillus Calmette–Guérin administration.

**Keywords:** Bacillus Calmette–Guérin, Granulomatous prostatitis, Prostate, Prostate imaging–reporting and data system

## INTRODUCTION

Granulomatous prostatitis (GP) is a benign inflammatory condition of the prostate, characterized by presence of granulomas.<sup>[1,2]</sup> It is a rare form of chronic prostatitis with incidences reported in literature ranging from 0.65% to 1.5% incidence of all inflammatory prostate lesions.<sup>[3–7]</sup> The etiology of GP is unclear; most cases are idiopathic. The leading hypothesis is the immune response to extra-ductal prostatic secretions, refluxed urine, bacteria, and colloidal contents trigger this cascade of events.<sup>[7,8]</sup> Existing data suggest increased incidence of GP in cases with recurrent urinary tract infections, prostate interventions including radical prostatectomy to core needle biopsy, and instillation of bacillus Calmette–Guérin (BCG) into the bladder.<sup>[3,9–11]</sup> GP can occur in normal or hyperplastic gland, or in carcinomatous prostate.<sup>[3,10]</sup>

On gross pathology, the prostate is firm to stony hard and cut sections show architectural distortion with formation of yellow granular nodules. Large nodular aggregates of histiocytes, epithelioid cells, multinucleated giant cells, and plasma cells are present on histopathology.<sup>[12]</sup>

Radiological features of GP overlap with those of prostate adenocarcinoma which can make diagnosis by imaging alone difficult. Lee *et al.*, in a retrospective study of 16 patients, found that in cases with GP, there is diffuse change involving >50% of the gland, with extracapsular extension and rim-enhancing areas.<sup>[13]</sup> GP should be considered as a differential diagnosis in the setting of recurrent urinary tract infection or prior BCG treatment.<sup>[13]</sup> Interestingly, Lee *et al.*, observed lower apparent diffusion coefficient (ADC) values in cases with GP, mean ADC value of  $702 \pm 79 \times 10^{-6} \text{ mm}^2/\text{s}$ .<sup>[13]</sup>

This is an open-access article distributed under the terms of the Creative Commons Attribution-Non Commercial-Share Alike 4.0 License, which allows others to remix, transform, and build upon the work non-commercially, as long as the author is credited and the new creations are licensed under the identical terms.

©2024 Published by Scientific Scholar on behalf of Journal of Clinical Imaging Science

While there is overlap of the imaging features with prostate adenocarcinoma, the following magnetic resonance imaging (MRI) characteristics and patterns are described in the literature and can suggest diagnosis of GP in the appropriate clinical setting. By T2-weighted imaging GP can present with diffuse or nodular pattern of low-signal intensity lesions, loss of transitional zone architecture, and in few cases presence of capsular irregularity.<sup>[13-16]</sup> On diffusion-weighted images (DWI), there is high-signal intensity with corresponding low signal on ADC.<sup>[13-16]</sup> Post-contrast imaging shows early diffuse enhancement with or without rim enhancement from caseous necrosis and abscess formation.<sup>[13-16]</sup> These imaging features are suggestive of the diagnosis; however, biopsy is typically necessary for confirmatory diagnosis.

Here, we present a case of GP in the setting of BCG therapy for bladder cancer.

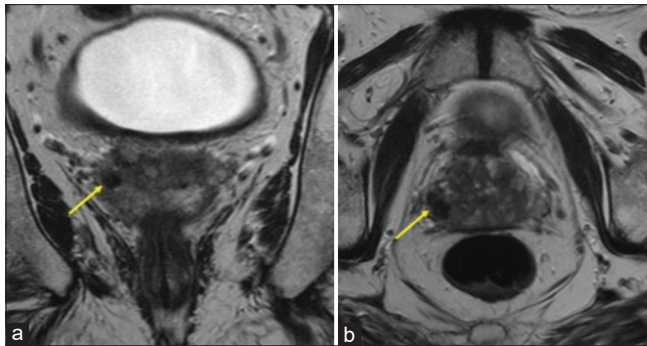


**Figure 1:** A 70-year-old male with bacillus Calmette–Guérin granulomatous prostatitis who presented with elevated prostate-specific agent. (a) Magnetic resonance imaging of the prostate with and without contrast, coronal T2-weighted image shows right prostate base 14 mm lesion (yellow arrow). (b) Axial T2-weighted image shows the lesion (yellow arrow) with low-signal intensity.

## CASE REPORT

### Clinical presentation

The patient is a 70-year-old male with medical history of low-grade bladder cancer (non-invasive low-grade papillary urothelial carcinoma) treated with intravesical BCG therapy (#12 cycles), last cycle administered 12 years before current presentation. On a regular follow-up visit, his prostate-specific agent (PSA) was elevated to 6.4 ng/mL. The patient denies a family history of prostate or urothelial cancer. The patient is a former smoker with eight pack years with smoking cessation following the diagnosis of bladder cancer.

### Imaging

Multiparametric prostate MRI (mpMRI) with and without contrast was performed, which showed multifocal lesions in the peripheral zone, the largest lesion in right base measured 14 mm in largest dimension, and most compatible with prostate imaging-reporting and data system (PI-RADS) 4 (High-clinically significant prostate cancer is likely to be present).<sup>[17-20]</sup> The smaller bilateral lesions ( $\leq 5$  mm) demonstrate imaging features most compatible with a PI-RADS 3 (Intermediate – the presence of clinically significant prostate cancer is equivocal) [Figures 1-3]. The lesions were assigned PI-RADS scores; however, GP was offered as an alternative diagnosis given the prior history of BCG therapy and multifocal, nodular distribution. Targeted tissue sampling was recommended.

On transrectal ultrasound, the prostate measured 41.7 mm  $\times$  48.9 mm  $\times$  27.7 mm (length, width, and height) with a calculated volume of 29.5 cubic cm. No hyperechoic or hypoechoic areas were visualized within.

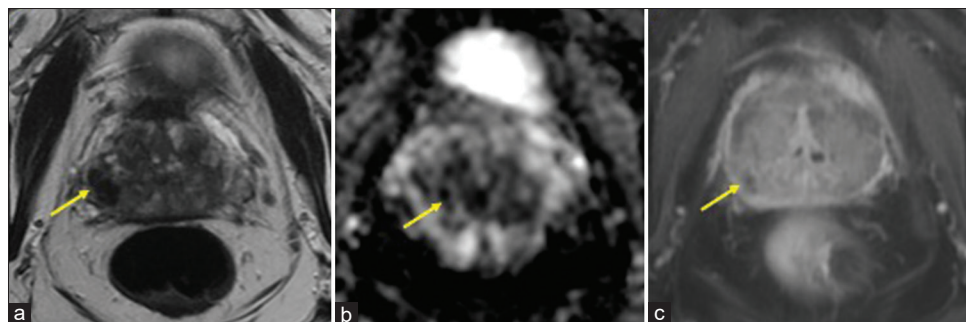


**Figure 2:** A 70-year-old male with bacillus Calmette–Guérin granulomatous prostatitis who presented with elevated prostate-specific agent. (a) Magnetic resonance imaging (MRI) of the prostate, axial T2-weighted imaging: By prostate imaging-reporting and data system (PI-RADS) criteria, the lesion's (yellow arrow) imaging features are most compatible with PI-RADS 4 (High-clinically significant prostate cancer is likely to be present). (b) MRI of the prostate, axial apparent diffusion coefficient: The right prostate base lesion (yellow arrow) restricts diffusion and demonstrates non-enhancing core. (c) MRI of the prostate, post contrast T1: By PI-RADS criteria, the lesion's (yellow arrow) imaging features are most compatible with PI-RADS 4 (High-clinically significant prostate cancer is likely to be present).

## Biopsy

Six random biopsies were obtained from the right and left portions of anteromedial, anterolateral, posteromedial, posterolateral, medial base, and lateral base of the prostate gland. Three additional biopsies were taken from the MRI-targeted lesions in the right base, left mid, and right anterior lobe. PSA density was 0.22. Patient tolerated the procedure without any complications. Targeted biopsy of the MRI lesion from right base, left mid, and right anterior lobe was reported as chronic prostatitis with granulomas, with atrophy and fibrosis, compatible with GP [Figure 4]. All submitted biopsy samples were negative for prostatic adenocarcinoma. In addition, random biopsies from different areas also revealed evidence of chronic prostatitis with granulomas and atrophy.

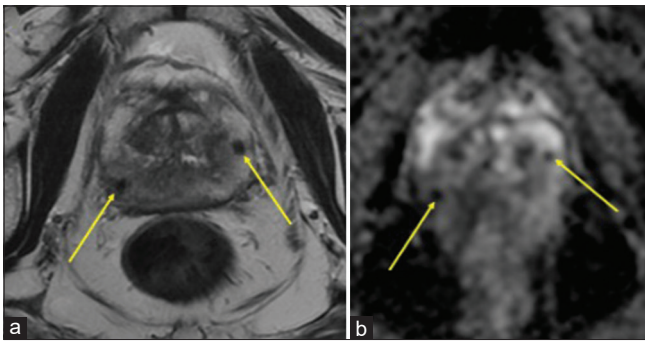


**Figure 3:** A 70-year-old male with bacillus Calmette–Guérin granulomatous prostatitis who presented with elevated prostate-specific antigen. (a) Magnetic resonance imaging of the prostate with and without contrast, axial T2-weighted image shows additional multifocal lesions (yellow arrows) in the peripheral zone, measuring 5 mm or less. No abnormal enhancement. (b) Apparent diffusion coefficient image shows imaging features most compatible with a Prostate Imaging-Reporting and Data System 3 (intermediate - the presence of clinically significant prostate cancer is equivocal) and the peripheral zone multifocal lesions (yellow arrows) seen in (a).

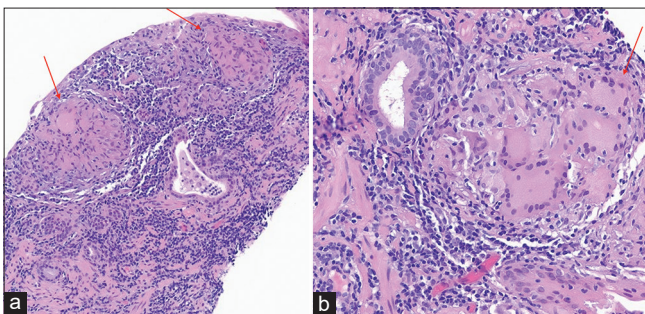


**Figure 4:** A 70-year-old male with bacillus Calmette–Guérin granulomatous prostatitis who presented with elevated prostate-specific antigen. (a) Hematoxylin and eosin (H&E) image at ×200 magnification shows well-formed epithelioid granulomas (red arrows) with a background of chronic inflammation. (b) H&E image at ×400 magnification shows epithelioid granuloma (red arrow) with multinucleated giant cells in a background of chronic inflammation.

## DISCUSSION

PI-RADS was developed by an internationally representative group involving the American College of Radiology, European Society of Urogenital Radiology, and AdMeTech Foundation. It provides a structured reporting scheme for mpMRI in the evaluation of suspected prostate cancer in treatment of naive prostate glands.<sup>[17]</sup> The use of PI-RADS does not contribute significantly to differentiate GP from malignancy. At most institutions, a PI-RADS score of 3 or greater prompts further evaluation with biopsy.

Symptomatically, patients present with fever, chills, urgency, frequency, and dysuria or maybe asymptomatic.<sup>[21]</sup> Clinically, patients with GP may present with an indurated prostate or a non-tender, palpable nodule adjacent to the prostate on digital rectal examination.<sup>[22,23]</sup> A history of intravesical BCG-therapy or recent urinary tract infection can indicate the need for imaging with a suspicion of GP. Clinical GP may present with normal to elevated serum PSA levels.<sup>[24]</sup> Increased PSA levels in the months post-BCG instillation are a frequent finding.<sup>[25]</sup> Although PSA is a screening marker found to be elevated in patients with prostatic carcinoma, it is non-specific and, further, evaluation is needed to differentiate the cause.<sup>[10,24]</sup>

### Pathologic features

The pathogenic mechanisms of GP are thought to be either direct infection or inflammation.<sup>[26]</sup> Intraprostatic reflux of BCG-contaminated urine from the bladder establishes the prostatic nidus and initiates the chronic inflammatory response, resulting in the formation of non-caseating or caseating granulomas within the prostate or periprostatic tissue, including the prostatic urethra.<sup>[27]</sup> Several microorganisms including tuberculosis, syphilis, brucellosis, viral, and fungal entities can cause GP. However, the infectious cause of BCG-induced GP is *Mycobacterium tuberculosis*.

Prostatic adenocarcinoma, non-specific GP, post-biopsy hemorrhage, benign prostatic hyperplasia nodules, and acute and chronic prostatitis can all mimic BCG-related GP.<sup>[24]</sup> Rarely, adenocarcinoma may coexist with GP.<sup>[26]</sup> Asymptomatic individuals do not require any specific treatment as GP is self-limited but tuberculostatic drugs may be initiated and systemic disease warrants the addition of anti-inflammatory drugs like prednisone.<sup>[26]</sup>

Histologically, epithelioid cell granulomas with Langhans giant cells may be seen. A prominence of epithelioid histiocytes or the appearance of a xanthogranulomatous pattern may require a follow-up immunohistochemical examination since this mimics adenocarcinoma. In cases of GP, immunohistochemistry reveals antibodies to CD68 (histiocyte marker) and in prostatic cancer, antibodies to cytokeratin 5/6 (basal cells) or cytokeratin AE1/AE3

(epithelial cells).<sup>[9]</sup> Acid-fast bacteria (AFB) staining may reveal *M. tuberculosis* or may be negative. Other special stains commonly do not detect any microorganisms.

### Radiologic features

Multiparametric MRI has become a commonly utilized imaging tool to assess the presence of clinically significant prostate cancer (Gleason 7 or greater). The typical mpMRI findings of GP are: (i) low-intensity signal on T2-weighted images, (ii) hyperintense signal on DWI, (iii) low-signal/values on ADC maps, and (iv) peripheral rim enhancement on contrast.<sup>[22,28,29]</sup>

A way to discern the diagnoses was proposed by Lee *et al.* by describing three different mpMRI patterns: A, B, or C.<sup>[13]</sup> Peripheral zone lesions with diffusion restriction and moderate to marked homogeneous enhancement on dynamic contrast-enhanced images were classified as type A. This pattern is indicative of highly cellular non-necrotic granulomas. The lesions with diffusion restriction and a poorly enhancing component were classified as type B. These are seen in necrotic GP with the central necrosis having a high-signal density on T2-weighted images and focal hyperintensity on high b-value images. A low-signal intensity on high b-value DWI ( $b = 1000 \text{ s/mm}^2$ ) is considered characteristic of type C. The suggested protocol is to use these findings alongside other diagnostic modalities and sequential monitoring on follow-up.<sup>[27,30]</sup>

Another study identified three main patterns on MRI-diffuse, nodular, and cystic with mural nodule.<sup>[31]</sup> A notched polygonal prostatic nodule is a diagnostic feature of GP. Sarkis *et al.* established the set of the prostatic imaging changes seen before and after BCG administration.<sup>[32]</sup> A comparative study with pre-operative PSA and prostate MRI can help rule out prostate carcinoma.<sup>[33]</sup> Gottlieb *et al.* recognized two-phased patterns of GP, acute and chronic, based on the temporal distribution of prostatic changes on mpMRI using the high-b-value sequence.<sup>[29]</sup>

Transrectal prostatic sonography may demonstrate nodular/diffuse hypoechoic areas in the prostate, which is a non-specific finding. Ultrasound examination only serves to complement the digital rectal examination and suspicious findings in the peripheral zone of the prostate must be followed by histological examination on biopsy.<sup>[21,23,34]</sup> Increased focal prostatic uptake on 2-deoxy-2-(fluoro-<sup>18</sup>F)-D-glucose positron-emission tomography-computed tomography (PET-CT) can be indicative of malignancy but in patients with a high degree of suspicion for GP, it is considered a benign finding.<sup>[35,36]</sup> PET-CT merely indicates hypermetabolic state of the tissue in GP.<sup>[37]</sup>

Based on MRI alone, GP and prostate cancer cannot be definitively distinguished since they share common

imaging features. Due to their overlapping features, biopsy is necessary for histologic confirmation, although the MRI findings can be suggestive in the setting of prior BCG administration. Therefore, if the biopsy and MRI findings are concordant, the information is critically useful in the event of future MRI examinations to avoid unnecessary re-targeting and re-biopsy of known foci of GP.

### CONCLUSION

A combination of clinical evaluation, imaging techniques like mpMRI, and histological examination can help in the accurate distinction between GP and prostate adenocarcinoma. Knowledge of GP and its features are important considerations for radiologists interpreting initial and follow-up prostate MRI examinations.

### Ethical approval

The Institutional Review Board approval is not required.

### Declaration of patient consent

The patient's consent is not required as the patient's identity is not disclosed or compromised.

### Financial support and sponsorship

Nil.

### Conflicts of interest

There are no conflicts of interest.

### Use of artificial intelligence (AI)-assisted technology for manuscript preparation

The authors confirm that there was no use of artificial intelligence (AI)-assisted technology for assisting in the writing or editing of the manuscript and no images were manipulated using AI.

### REFERENCES

1. Srigley JR. Benign mimickers of prostatic adenocarcinoma. *Modern Pathol* 2004;17:328-48.
2. James D. A clinicopathological classification of granulomatous disorders. *Postgrad Med J* 2000;76:457-65.
3. Shanggar K, Zulkifli MZ, Razack AH, Dublin N. Granulomatous prostatitis: A reminder to clinicians. *Med J Malaysia* 2010;65:21-2.
4. Punia RP, Mohan H, Bawa AS. Granulomatous prostatitis-an infrequent diagnosis. *Indian J Urol* 2002;19:16.
5. Stillwell TJ, Engen DE, Farrow GM. The clinical spectrum of granulomatous prostatitis: A report of 200 cases. *J Urol* 1987;138:320-3.

6. Kumbar R, Dravid N, Nikumbh D, Patil A, Nagappa KG. Clinicopathological overview of granulomatous prostatitis: An appraisal. *J Clin Diagn Res* 2016;10:EC20-3.
7. Mohan H, Bal A, Punia RP, Bawa AS. Granulomatous prostatitis--an infrequent diagnosis. *Int J Urol* 2005;12:474-8.
8. Oppenheimer JR, Kahane H, Epstein JI. Granulomatous prostatitis on needle biopsy. *Arch Pathol Lab Med* 1997;121:724-9.
9. Val-Bernal JF, Zaldumbide L, Garijo MF, González-Vela MC. Nonspecific (idiopathic) granulomatous prostatitis associated with low-grade prostatic adenocarcinoma. *Ann Diagn Pathol* 2004;8:242-6.
10. Bahnson RR. Elevation of prostate specific antigen from bacillus Calmette-Guérin-induced granulomatous prostatitis. *J Urol* 1991;146:1368-9.
11. Alexander RB, Mann DL, Borkowski AA, Fernandez-Vina M, Klyushnenkova EN, Kodak J, *et al.* Granulomatous prostatitis linked to HLA-DRB1\* 1501. *J Urol* 2004;171:2326-9.
12. Rosai J. Male reproductive system, prostate and seminal vesicles. In: Ackerman's surgical pathology. Netherlands: Elsevier; 1996. p. 1221-56.
13. Lee SM, Wolfe K, Acher P, Liyanage SH. Multiparametric MRI appearances of primary granulomatous prostatitis. *Br J Radiol* 2019;92:20180075.
14. Barentsz J, Richenberg J, Clements R, Choyke P, Verma S, Villeirs G, *et al.* ESUR prostate MR guidelines 2012. *Eur Radiol* 2012;22:746-57.
15. Weinreb JC, Barentsz JO, Choyke PL, Cornud F, Haider MA, Macura KJ, *et al.* PI-RADS prostate imaging – reporting and data system: 2015, version 2. *Eur Urol* 2016;69:16-40.
16. Yu A, Badve C, Ponsky L, Pahwa S, Dastmalchian S, Rogers M, *et al.* Development of a combined MR fingerprinting and diffusion examination for prostate cancer. *Radiology* 2017;283:729-38.
17. American College of Radiology. Prostate imaging reporting and data system (PI-RADS) version 2.1. Available from: <https://www.acr.org/-/media/acr/files/rads/pi-rads/pirads-v2-1.pdf> [Last accessed on 2022 Jul 25].
18. Westphalen AC, Rosenkrantz AB. Prostate imaging reporting and data system (PI-RADS): Reflections on early experience with a standardized interpretation scheme for multiparametric prostate MRI. *Am J Roentgenol* 2014;202:121-3.
19. Röthke M, Blondin D, Schlemmer HP, Franiel T. PI-RADS-Klassifikation: Strukturiertes befundungsschema für die MRT der prostata. *RÖFO* 2013;185:253-61.
20. Rosenkrantz A, Kim S, Lim R, Hindman N, Deng F, Babb J, *et al.* Prostate cancer localization using multiparametric MR imaging: Comparison of prostate imaging reporting and data system (PI-RADS) and likert scales. *Radiology* 2013;269:482-92.
21. Bude R, Bree RL, Adler RS, Jafri SZ. Transrectal ultrasound appearance of granulomatous prostatitis. *J Ultrasound Med* 1990;9:677-80.
22. Ambe Y, Nakamura M, Shirakawa N, Inatsu H, Amakawa R, Inoue Y, *et al.* Granulomatous prostatitis with high suspicion of prostatic adenocarcinoma on radiological imaging. *IJU Case Rep* 2021;4:247-9.
23. Rifkin M, Tessler F, Tublin M, Ross J. US case of the day. Granulomatous prostatitis resulting from BCG therapy. *Radiographics* 1998;18:1605-7.
24. Speights VO Jr, Brawn PN. Serum prostate specific antigen levels in non-specific granulomatous prostatitis. *Br J Urol* 1996;77:408-10.
25. Sauvat L, Lhermite Q, Desplechain C, Long B, Vidal M. An ambivalent prostate nodule after Bacillus Calmette-Guérin therapy. *Idcases* 2021;26:e01338.
26. Bilsen M, van Meijgaarden K, de Jong H, Joosten S, Prins C, Kroft L, *et al.* A novel view on the pathogenesis of complications after intravesical BCG for bladder cancer. *Int J Infect Dis* 2018;72:63-8.
27. Lee S, Oh YT, Kim HM, Jung DC, Hong H. Imaging patterns of Bacillus Calmette-Guérin-related granulomatous prostatitis based on multiparametric MRI. *Korean J Radiol* 2022;23:60-7.
28. Kawada H, Kanematsu M, Goshima S, Kondo H, Watanabe H, Noda Y, *et al.* Multiphase contrast-enhanced magnetic resonance imaging features of Bacillus Calmette-Guérin-induced granulomatous prostatitis in five patients. *Korean J Radiol* 2015;16:342.
29. Gottlieb J, Princenthal R, Cohen M. Multi-parametric MRI findings of granulomatous prostatitis developing after intravesical Bacillus Calmette-Guérin therapy. *Abdom Radiol (NY)* 2017;42:1963-7.
30. Crocetto F, Barone B, De Luca L, Creta M. Granulomatous prostatitis: A challenging differential diagnosis to take into consideration. *Future Oncol* 2020;16:805-6.
31. Suzuki T, Takeuchi M, Naiki T, Kawai N, Kohri K, Hara M, *et al.* MRI findings of granulomatous prostatitis developing after intravesical Bacillus Calmette-Guérin therapy. *Clin Radiol* 2013;68:595-9.
32. Sarkis J, Nawfal G, El-Haddad E, Tayeh G, Mahfoud N, Sarkis P. Comparative prostate MRI before and after chronic granulomatous prostatitis following intravesical bacillus Calmette-Guérin therapy. *Future Sci OA* 2021;7:FSO637.
33. Wang M, Wang Z, Han C, Xu Y, Yu X, Kang W, *et al.* The role of prostate-specific antigen and multiparametric magnetic resonance imaging in the diagnosis of granulomatous prostatitis induced by intravesical Bacillus Calmette-Guérin vaccine therapy in patients with nonmuscle invasive bladder cancer. *J Cancer Res Ther* 2021;17:625.
34. Rubenstein J, Swayne L, Magidson J, Furey C. Granulomatous prostatitis: A hypoechoic lesion of the prostate. *Urol Radiol* 1991;13:119-22.
35. Wilkinson C, Chowdhury F, Scarsbrook A, Smith J. BCG-induced granulomatous prostatitis-an incidental finding on FDG PET-CT. *Clin Imaging* 2012;36:413-5.
36. Ilgan S, Koca G, Gundogdu S. Incidental detection of granulomatous prostatitis by F-18 FDG PET/CT in a patient with bladder cancer. *Clin Nucl Med* 2009;34:613-4.
37. Kim CY, Lee SW, Choi SH, Son SH, Jung JH, Lee CH, *et al.* Granulomatous prostatitis after intravesical Bacillus Calmette-Guérin instillation therapy: A potential cause of incidental F-18 FDG uptake in the prostate gland on F-18 FDG PET/CT in patients with bladder cancer. *Nucl Med Mol Imaging* 2015;50:31-7.

**How to cite this article:** Hegde S, Lakhani DA, Prisneac I, Markovich B. Granulomatous prostatitis following Bacillus Calmette-Guérin therapy. *J Clin Imaging Sci.* 2024;21:39. doi: 10.25259/JCIS\_47\_2023